Vasopressin casts light on the suprachiasmatic nucleus

Takahiro Tsuji[1], Andrew J. Allchorne[1], Meng Zhang[2], Chiharu Tsuji[1], Vicky A. Tobin[1], Rafael Pineda[1], Androniki Raftogianni[3], Javier E. Stern[2] (iD), Valery Grinevich[3], Gareth Leng[1] and Mike Ludwig[1] (iD)

[1]*Centre for Integrative Physiology, University of Edinburgh, Edinburgh, UK*
[2]*Department of Physiology, Augusta University, Augusta GA USA*
[3]*Schaller Research Group on Neuropeptides, German Cancer Research Centre DKFZ, Central Institute of Mental Health, and University of Heidelberg, Heidelberg, Germany*

The Journal of Physiology

Key points

- A subpopulation of retinal ganglion cells expresses the neuropeptide vasopressin.
- These retinal ganglion cells project predominately to our biological clock, the suprachiasmatic nucleus (SCN).
- Light-induced vasopressin release enhances the responses of SCN neurons to light.
- It also enhances expression of genes involved in photo-entrainment of biological rhythms.

Abstract   In all animals, the transition between night and day engages a host of physiological and behavioural rhythms. These rhythms depend not on the rods and cones of the retina, but on retinal ganglion cells (RGCs) that detect the ambient light level in the environment. These project to the suprachiasmatic nucleus (SCN) of the hypothalamus to entrain circadian rhythms that are generated within the SCN. The neuropeptide vasopressin has an important role in this entrainment. Many SCN neurons express vasopressin, and it has been assumed that the role of vasopressin in the SCN reflects the activity of these cells. Here we show that vasopressin is also expressed in many retinal cells that project to the SCN. Light-evoked vasopressin release contributes to the responses of SCN neurons to light, and enhances expression of the immediate early gene c-*fos* in the SCN, which is involved in photic entrainment of circadian rhythms.

Introduction

The suprachiasmatic nucleus (SCN) of the hypothalamus is the circadian pacemaker of the mammalian brain, orchestrating diurnal cycles in activity, hormone secretion and other physiological variables (Reppert & Weaver, 2002; Hastings *et al.* 2003; Froy, 2011; Albrecht, 2012) according to an intrinsic circadian rhythmicity of neuronal activity and gene expression. Light entrains the endogenous oscillator in the SCN, synchronizing it with the day–night cycle (Golombek & Rosenstein, 2010), and in mammals information about ambient light intensity originates from a small subset of retinal ganglion cells (RGCs) that are intrinsically photosensitive (Masland, 2001; Hattar *et al.* 2002; Schmidt *et al.* 2011), rather than from the rods and cones that are responsible for visual imaging. These intrinsically photosensitive RGCs express the photopigment melanopsin (Lucas, 2013) and use the

neurotransmitter glutamate (Marc & Jones, 2002); they project to the SCN to mediate circadian photo-entrainment. This neural circuit is independent of conventional retinal phototransduction, since photic entrainment persists in functionally blind transgenic mice lacking rods and cones (Berson *et al.* 2002).

Changes in day length require progressive adjustments of circadian rhythms, but it would be counter-adaptive to reset a rhythm to *any* unexpected light signal. Our experience of jet lag reflects the resistance of our bodily rhythms to abrupt changes (LeGates *et al.* 2014). Accordingly, in animals, a flash of light close to the end of the night is more likely to result in a phase shift of circadian rhythms than one given earlier. Such light pulses induce expression of a set of immediate-early genes in the SCN, and the ability of light to re-entrain circadian rhythms correlates well with the induction of these genes (Rusak *et al.* 1993; Kornhauser *et al.* 1996; Porterfield & Mintz, 2009). Thus a key question is, how can a light pulse trigger gene expression and re-entrain circadian rhythms at some times but not at others? Because the neurones in the SCN display circadian rhythms in gene expression that are maintained even in constant darkness, one possible answer is that these genes regulate intrinsic neuronal excitability, with the consequence that the SCN neurons are only fully responsive to light signals at certain stages of the light–dark cycle. Recent findings indicate that the neuropeptide vasopressin may have a critical role in this process. Transgenic vasopressin V1a receptor knockout mice show damped circadian activity rhythms (Li *et al.* 2009), and, interestingly, such mice are resistant to 'jet lag'. In these mice, light pulses immediately re-entrain circadian rhythms (Yamaguchi *et al.* 2013).

Vasopressin is involved in diverse physiological and behavioural processes; vasopressin secreted from the pituitary gland is essential for fluid and electrolyte balance, while vasopressin released within the brain has many other roles, including in social behaviour, in aggression and in behavioural rhythms (Bielsky *et al.* 2005; Ludwig & Leng, 2006; Donaldson & Young, 2008; Bosch & Neumann, 2012; Mieda *et al.* 2015). Vasopressin is expressed in the dorso-medial SCN, and is an important output; its secretion into the cerebrospinal fluid (CSF) peaks in the early morning and declines by late afternoon (Kalsbeek *et al.* 2010). The targets for vasopressin released from the SCN include vaso-pressin cells in other parts of the hypothalamus, including those in the supraoptic and paraventricular nuclei that regulate diverse physiological processes including water intake and behaviours (Trudel & Bourque, 2010; Gizowski *et al.* 2016).

The vasopressin cells in the dorsomedial SCN are not direct recipients of retinal signals; most of the projections from the retina innervate the ventrolateral SCN, which contains other neuropeptides, including vasoactive intestinal peptide and gastrin-releasing peptide (Antle *et al.* 2009). Here we show that neurons in the ventrolateral SCN are densely innervated by vasopressin-expressing retinal ganglion cells (VP-RGCs), and that more vasopressin is released in response to light at the end of subjective night than at the end of sub-jective day. Thus neurons in the ventrolateral SCN both control the output of vasopressin from the SCN by their innervation of vasopressin cells in the dorsomedial SCN, and are themselves regulated by vasopressin inputs from the retina.

Methods

Ethical approval

Procedures conducted in the UK were approved by the local Ethics Committee and the UK Home Office under the Animals (Scientific Procedures) Act 1986. Experiments in Germany were approved by the Committee on Animal Health and Care of the local governmental body and performed in strict compliance with the EEC recommendations for the care and the use of laboratory animals (86/609/CEE). Experiments in the USA were performed according to institutional guidelines and approval by the Animal Care and Use Committees of the Georgia Regents University.

Animals

Experiments were performed on adult male and female wild-type Sprague–Dawley and transgenic rats (250–350 g), housed under controlled conditions (12 h light–12 h dark, 21°C) with free access to food and water. Most of the immunohistochemistry was carried out on a homozygous line of transgenic rats expressing a vasopressin–enhanced green fluorescent protein (eGFP) fusion gene (Ueta *et al.* 2005).

PCR

Female wild-type rats, 22 weeks old, were used to collect supraoptic nucleus and retina tissue. Total RNA was iso-lated using TRIzol Reagent (Life Technologies, Carlsbad, CA, USA). cDNA was synthesized from 1.5 μg of total RNA using the Transcriptor High Fidelity cDNA Synthesis Kit (Roche Diagnostics GmbH, Mannheim, Germany) according to the manufacturer's protocol. The PCR was carried out in a 25 μl reaction volume using Go Taq G2 Green Master Mix (Promega Corp., Madison, WI, USA) and 5, 1 or 0.1 μl of cDNA solution was used in each reaction mixture. PCR was performed on a Gene Amp PCR System 9700 (Life Technologies) using the following conditions: 1 cycle of 94°C for 30 s followed by 30 cycles of 94°C for 30 s, 56°C for 45 s and 72°C for 1 min, with a

final extension step at 72°C for 7 min. PCR products were loaded on the 2% agarose gel and stained with SYBR Safe DNA Gel Stain (Life Technologies). The primer sequences have been published previously (Dijk *et al.* 2004; Gainer *et al.* 2011).

Tissue collection and processing

Rats were terminally anaesthetized and perfusion-fixed with 4% paraformaldehyde (PFA) following a heparinized saline flush, and post-fixed and cryoprotected as previously described (Tobin *et al.* 2010). The eyes were enucleated and placed in 0.1 M phosphate buffer (PB) during the heparinized saline flush before transcardial perfusion with PFA. The cornea was cut around the outer edge of the iris to remove the lens and vitreous humour and the eyecups were either placed in 4% PFA solution for 5 min and the retina gently removed and placed back in 4% PFA for 20 min or each eyecup was left in 4% PFA solution for 2 h. Some retinas were fixed in a solution of 4% PFA + 1% glutaraldehyde but otherwise processed as described above. Tissue was then stored at 4°C in 10% sucrose, then placed in 20% sucrose solution for 120 min and finally in 30% sucrose for 12–48 h, until the tissues had sunk to the bottom of the vials. In eyes that were required for coronal or transverse sections, the tissues were then placed in Tissue-Tek CRYO-OCT (optimal cutting temperature compound) embedding matrix (Fisher Scientific, Loughborough, UK)-filled cryo-molds (Sakura Finetek UK Ltd, Thatcham, UK) and gently manipulated to open up and be in the appropriate orientation and then snap-frozen on powdered dry ice. The retinas or eyecups were stored at −20°C until 16 μm sections were cut at −15°C on a cryostat. These sections were thaw-mounted onto SupraFrost slides, allowed to air-dry for 10 min before being stored at −20°C until they were processed for fluorescence immunocytochemistry. For retinal flat mounts, three to four incisions were made from the perimeter of the retina almost to the centre to allow the retina to be gently flattened. The flat-mounts were stored in 0.1 M PB until used for immunohistochemistry. After transcardial perfusion, the brains were removed and placed in a 2% PFA–15% sucrose solution overnight and transferred to 30% sucrose until the tissue had sunk. Coronal 40 μm sections were cut using a freezing microtome.

Immunohistochemistry

For brain sections and rat retina flat mounts, immunohistochemistry was conducted using a free-floating technique. For retina sections, immunohistochemistry was conducted on the slides either in slide-mailers (Fisher Scientific UK) or after the sections on each slide were outlined with hydrophobic ink (ImmEdge, Vector

Laboratories, Peterborough, UK) and thereafter kept horizontal in a light-proofed humid chamber. For each of these techniques, the sections were thoroughly rinsed in 0.1 M PB and incubated in 0.1 M glycine in 0.1 M PB for 30 min at room temperature. For immunohistochemistry involving exposure to a biotinylated secondary and fluorescently tagged streptavidin, sections were blocked for endogenous biotin by incubating them first in 0.01% avidin in 0.1 M PB for 30 min, washing and then incubating in 0.001% biotin in 0.1 M PB for 30 min. After washing, sections were incubated for 60 min in a blocking buffer consisting of 3–5% normal serum (matched to the host of secondary animal) +1% bovine serum albumin (BSA) + 0.1% Triton X-100 diluted in 0.1 M PB. If the primary antibody was raised in goat, BSA was not used in either the blocking buffer or the antibody-diluting buffer. The sections were incubated with primary antibodies (Table 1) diluted in the blocking buffer. The primary antibodies were applied for 1–5 days at room temperature for the first day and thereafter at 4°C. After washing in 0.1 M PB, sections were incubated for 60 min with secondary antibodies and then washed in 0.1 M PB. Sections exposed to biotinylated secondary antibodies were then incubated for 60 min with fluorescently labelled streptavidin conjugate (1:1000). Both secondary antibodies and fluorescently labelled streptavidin were diluted in 0.1 M PB + 0.03% Tween. After further washing, sections were incubated in 4′,6-diamidino-2-phenylindole (DAPI, 1:33 000, Life Technologies Ltd, UK) for 5 min at room temperature, washed and coverslipped using either a Mowiol 4–88 (Calbiochem, San Diego, CA, USA) mounting medium, supplemented with 2.5% 1,4-diazabicyclo[2.2.2]octane (DABCO, Sigma-Aldrich) or Prolong Gold (Life Technologies Ltd, UK). No fluorescent labelling was detected when primary antibodies were omitted or when the primary antibodies (Table 2) were incubated with a fivefold (w/v) control immunogen before being exposed to the tissue sections (the latter control was conducted whenever a control peptide was available from the supplier of that primary antibody). Most antibody suppliers provided Western blot analysis showing the antibody detecting protein in a single band of appropriate size.

Microscopy

Fluorescence signals were acquired either using a Nikon AIR confocal or a Zeiss LSM510 Axiovert confocal laser scanning microscope. In either case, the images were acquired at 1024 × 1024 pixels, using a Nikon Plan Apochromat 1.4 NA ×60 oil-immersion objective or a Zeiss Plan NeoFLUAR 1.4 NA ×63 oil-immersion objective, respectively. In all cases, emissions for each fluorophore were obtained consecutively to avoid channel cross-talk. Those images taken throughout each cell

Table 1. Primary antibodies used for retina and SCN immunohistochemistry

Primary antibody	Cat. no.	Supplier	Dilution	Host
eGFP	AB3080	Millipore, UK	1:1000	Rabbit
eGFP	MAB3580	Millipore, UK	1:1000	Mouse
Venus (GFP and YFP)	ab13970	Abcam, UK	1:15000	Chicken
tdTomato	362496	Clontech	1:500	Rabbit
Gastrin releasing peptide	ab43834	Abcam, UK	1:500	Rabbit
Vasoactive intestinal peptide	20077	Immunostar, Newmarket Scientific, UK	1:500	Rabbit
Melanopsin	AB19306	Abcam, UK	1:100	Rabbit
Neuropeptide Y	22940	Immunostar, Newmarket Scientific, UK	1:500	Rabbit
Somatostatin	20067	Immunostar, Newmarket Scientific, UK	1:500	Rabbit
Vasopressin	PS41	Professor H. Gainer (NIH, Bethesda, MD, USA)	1:1000	Mouse
Vasopressin	PC234L	Merck Chemicals Ltd, UK	1:200	Rabbit
Calbindin D-28K	300	Swant, Switzerland	1:500	Mouse
Calretinin	7699/3H	Swant, Switzerland	1:500	Rabbit
Parvalbumin	24428	Immunostar, Newmarket Scientific, UK	1:500	Rabbit
Glutamate decarboxylase 65/67	ADI-MSA-225	Enzo Life Sciences (UK) Ltd, Exeter, UK	1:1000	Mouse
Vesicular glutamate transporter 2	135404	Synaptic Systems, Germany	1:1000	Guinea pig
Glycine	AB5020	Millipore, UK	1:100	Rabbit
Tyrosine hydroxylase	AB152	Millipore, UK	1:1000	Rabbit
Dopamine β-hydroxylase	AB1585	Millipore, UK	1:2000	Rabbit
Choline acetyltransferase	AB144P	Millipore, UK	1:1000	Goat
Fos	PC38	Millipore, UK	1:20000	Rabbit
Fos	226003	Synaptic Systems, Germany	1:100000	Rabbit

Table 2. Secondary and visualization reagents used for retina and SCN

Secondary antibody and visualization	Cat. no.	Supplier	Dilution	Host
Secondary antibody				
Biotin–anti-rabbit IgG	BA-1100	Vector Laboratories Ltd, UK	1:500	Horse
Biotin–anti-mouse IgG	BA-2001	Vector Laboratories Ltd, UK	1:500	Horse
Biotin–anti-guinea pig IgG	BA-7000	Vector Laboratories Ltd, UK	1:500	Goat
Biotin–anti-rabbit IgG	BA-1000	Vector Laboratories Ltd, UK	1:500	Goat
Biotin–anti-mouse IgG	BA-9200	Vector Laboratories Ltd, UK	1:500	Goat
Alexa 488 anti-chicken	A11039	Life Technologies, UK	1:500	Goat
Biotin–anti-chicken IgY	703-066-155	Stratech Scientific Ltd, UK	1:500	Donkey
Visualized with				
Streptavidin, Alexa Fluor 488 conjugate	S-11223	Life Technologies, UK	1:500	
Streptavidin, Alexa Fluor 555 conjugate	S-21381	Life Technologies, UK	1:500	
Streptavidin, Alexa Fluor 647 conjugate	S-21374	Life Technologies, UK	1:500	

at Nyquist sampling rates were deconvolved using Huygens software (Scientific Volume Imaging, Hilversum, Netherlands) and all images were analysed using NIH ImageJ software (v1.48) and figures constructed using Microsoft PowerPoint.

Cloning of rAAV vectors and virus production

In addition to tissue from transgenic rats, for morphological studies we used tissue from wild-type rats given bilateral intravitreal injections (under iso-flurane anaesthesia) of a recombinant adeno-associated virus (rAVV) that caused the expression of Venus or tdTomato under the control of the vasopressin promoter. The conserved promoter region of the vasopressin gene, chosen using the software BLAT from UCSC (http://genome.ucsc.edu/cgi-bin/hgBlat) was subcloned into an rAAV2 backbone carrying ampicillin resistance. It comprises a 1.9 kb sequence stretch (revealed by BLAT) that allows for cell-specific expression in hypothalamic vasopressin neurons. Venus or tdTomato was introduced to the plasmid as the gene of interest. Production of chimeric virions (recombinant Adeno-associated virus 1/2; rAAV 1/2) was described previously (Knobloch

et al. 2012). Briefly, human embryonic kidney cells 293 (AAV293; Agilent, Santa Clara, CA, USA; cat. no. 240073) were calcium phosphate-transfected with the recombinant AAV2 plasmid and a 3-helper system (During *et al.* 2003). rAAV genomic titres were determined with QuickTiter AAV Quantitation Kit (Cell Biolabs, Inc., San Diego, CA, USA) and were $\sim 10^{13}$ genomic copies per millilitre.

Rats were anaesthetized by medetomidine–ketamine injection and placed in a tiltable stereotaxic frame. A few drops of phenylephrine chlorhydrate and tropicamide (Mydrin-P®) to induce mydriasis, oxybuprocaine chlorhydrate (Benoxil® 0.4%) for additional local anaesthesia, and ofroxacin (Tarivid® 0.3%) antibiotic were administered into each eye. The head was tilted with its left or right eye uppermost. Intravitreal injections were performed as described by Chiu *et al.* (2007). Using a very fine needle (33G, Heraeus, Kulzer Japan Co., Ltd, Tokyo, Japan) attached to a 0.025 ml Hamilton syringe (Microliter™ 702), a small puncture was made in the region of the limbus and the needle was lowered into the vitreous using a micromanipulator. Two to five micro-litres of rAAV was intravitreally injected into both eyes of transgenic or wild-type rats. The needle was left in position for 30–60 s and then withdrawn slowly. The procedure was repeated on the other side of the same eye before being repeated on the other eye. Injections were performed under a dissecting microscope to ensure correct positioning of the needle and to monitor loss of fluid from the eye. Intravitreal injections were performed by a trained ophthalmologist. Virally transfected rats were left for 2 weeks before transcardial perfusion.

Retrograde tracing

In 12 eGFP rats under isoflurane anaesthesia, 50–100 nl of the retrograde tracer (Red-Retrobeads, Lumafluor Inc., Naples, FL, USA, or Fluorogold, Sigma-Aldrich) was microinjected stereotaxically in the left SCN (bregma −1.1, lateral +0.3, depth 8.6 mm from dura), inter-geniculate leaflet (IGL; bregma −4.5, lateral +4.0, depth 5.5 mm from dura), olivary pretectal nucleus (OPt; bregma −4.7, lateral 1.3, depth 4.4 mm from dura) or bilaterally into the left and right superior colliculus (bregma −5.3 mm, lateral 1.5 mm, depth 4.8 mm from dura) (Paxinos & Watson, 2006) over 20 min. One week later, rats were perfused transcardially with 4% PFA and brains and retinas were processed for immunohistochemistry.

Fos expression

The effects of light on Fos expression on eGFP-positive RGCs and the SCN was evaluated in eGFP rats fixed by transcardial perfusion during the day (noon) or night after light exposure (1000 lux, for 1 h, 2 h before the end of the night). Standard immunocytochemistry was performed on floating retinal flat mounts or SCN sections using a polyclonal antibody raised in rabbit against the N-terminal amino acids 4–17 of the protein product of human c-*fos* (PC38, Millipore, UK). For double immuno-cytochemistry, a polyclonal antibody raised in chicken against eGFP (Abcam UK) was used. Antibody-antigen complexes were visualized by using ABC methods with a Vector stain elite kit (Vector Laboratories, Peterborough, UK) intensified with nickel-intensified diaminobenzidine (Ni-DAB; single immunocytochemistry) or with DAB only (double immunocytochemistry). Fos-positive nuclei and the percentage of activated cells were counted in the SCN at the level of maximal cross-sectional area by an observer blind to the treatment group.

Intracerebroventricular infusion of vasopressin V1a antagonist

Wild-type rats were implanted with a left lateral ventricular brain infusion cannula (Alzet BIK2, Charles River Ltd, Margate, UK) under isoflurane anaesthesia via a burr hole in the skull drilled 0.6 mm posterior to and 1.6 mm lateral to bregma (Paxinos & Watson, 2006). The cannula was secured in place using dental cement glued to two stainless steel screws driven into the skull and then connected via polythene tubing to a subcutaneous osmotic minipump (Alzet 2001; Cupertino, CA, USA). The pumps were prepared as in the manufacturer's instructions and filled with a vasopressin V1a receptor antagonist ($d(CH_2)_5Tyr(Me)^2AVP$; (Kruszynski *et al.* 1980) or aCSF and set to deliver at a rate of 416 ng h^{-1}, for 3 days ($n = 5$–7/group). This antagonist binds similarly to V1a and V1b receptors, and the dose is about twice that used previously by Subburaju & Aguilera (2007), who delivered 230 ng h^{-1} for 28 days and showed effectiveness at blocking the effects of exogenous vasopressin. Rats were housed singly and, on the day of experiment, were moved into a brightly lit laboratory (1000 lux) and placed into empty clear cages for 1 h. They were then terminally anaesthetized for tissue fixation (see above).

In vivo electrophysiology

Urethane (ethyl carbamate 1.25 g kg^{-1}, I.P.)-anaesthetized adult male wild-type rats were tracheotomized and the area below the SCN was exposed using a transpharyngeal approach (Ludwig *et al.* 2002; Saeb-Parsy & Dyball, 2003). An injection cannula was placed into the third ventricle (coordinates: 0.6 mm caudal to bregma, 1.5 mm lateral to midline, 5 mm deep) (Paxinos & Watson, 2006) for I.C.V. drug administration, and in some experiments a bipolar stimulating electrode was placed onto the exposed optic nerve, as above, contralateral to the recording side. Recordings were made from single cells in the SCN

using a glass microelectrode (tip diameter ~1 μm) filled with 0.9% NaCl; firing rates were recorded using Spike2 software and CED 1401 interface (Cambridge Electronic Design, Cambridge, UK) on a PC. The spontaneous activity of each SCN neuron was recorded for at least 5 min before treatment. Trains of stimuli (matched biphasic pulses; 1 ms pulses, 1 mA peak-to-peak; 50 Hz for 0.5 s, every 1 min) were applied to the contralateral optic nerve. Light was applied at 1500 lux for 5 s at 1 min intervals after the rats were held in dark conditions with eyes covered with aluminum foil. Electrical or light stimulation was repeated before, during and after injection of a vasopressin antagonist into the third ventricle, 2–3 mm caudal to the recording site. The injection cannula was back-filled with vasopressin V1a antagonist (40 ng in 2 μl aCSF; Tobin *et al.* 2010) followed by 2 μl of aCSF to prevent diffusion of antagonist into the SCN; in tests, the first injection of 2 μl was thus of aCSF, followed 10 min later with an injection of antagonist. Responses to light were averaged over 10–20 presentations; responses to antagonist began ~5 min after injection so the average of responses after this time was taken. Only one cell was tested in each experiment. One of the cells tested with the antagonist was not tested with aCSF; in that experiment a different cell had been tested with aCSF with no response (not shown) but was lost before the antagonist could be injected.

In vitro electrophysiology

eGFP rats were terminally anaesthetized with pentobarbital (50 mg kg^{-1}) and retinas dissected out as described previously (Schmidt & Kofuji, 2011). Retinas were treated with enzymes by adding collagenase and hyaluronidase (Worthington Chemicals) to Ames' solution for 10 min in a 95% O$_2$–5% CO$_2$ environment, shaken gently before being washed 3 times in carbon-saturated Ames' solution and stored in dark for at least 1 h before being moved to the recording chamber. Retina flat mounts were superfused with Ames' solution (30–32°C) at 3 ml min^{-1}. Conventional whole-cell patch-clamp recordings, using a potassium gluconate-based internal solution, were obtained as previously described (Son *et al.* 2013). Some neurons were intracellularly labelled with Alexa Fluor 555 (100 μM) or biocytin (1%). Recordings were obtained from eGFP-labelled VP-RGCs neurons. For bath-applied drugs, mean firing activity and membrane potential values were calculated from a 2 min period before drug application and in a 2 min period around the peak effect.

Microdialysis

In wild-type rats, the brain region above the SCN was exposed by the transpharyngeal approach under urethane anaesthesia (ethyl carbamate 1.25 g kg^{-1}, I.P.) as previously described (Ludwig *et al.* 2002). An in-house designed U-shaped microdialysis probe (molecular mass cut-off of 6 kDa, Fleaker® hollow fibre, Spectrum Medical Inc., Los Angeles, CA, USA) was positioned into the left SCN after opening of the meninges. After implantation, there was an equilibration period of at least 1 h before six consecutive 30 min dialysis samples were collected. The samples were frozen and stored at -20°C until assay for vasopressin. After two 30 min baseline periods, a stimulating electrode (Clarke Electromedical, Edenbridge, Kent, UK, SNEX-200X) placed onto the optic nerve closely behind the right eye was set to deliver trains of matched biphasic pulses (0.1 ms, 1 mA peak-to-peak; 50 Hz for 5 s, every 1 min for 30 min). In other experiments, light was applied (1 min on–1 min off for 30 min) to the eye contralateral to the recording site using a portable surgical light (1500 lux) at early morning or late evening during the third sampling period. For the early morning measurements, rats were anaesthetized at zeitgeber time (ZT) 0, and kept in the dark (covering the eyes with aluminium foil) before stimulating with light at ZT4. For the late evening measurements, rats were anaesthetized at ZT9 and then kept in the dark (covering the eyes with aluminium foil) before stimulating with light at ZT12. The SCN was dialysed with aCSF (pH 7.2, composition in mM: NaCl 138, KCl 3.36, NaHCO$_3$ 9.52, Na$_2$HPO$_4$ 0.49, urea 2.16, CaCl$_2$ 1.26, MgCl$_2$ 1.18) at 3 μl min^{-1}). At the end of each experiment, during microdialysis sample period 6, a modified aCSF containing 150 mM KCl plus 100 μM veratridine was retrodialysed into the SCN to trigger vasopressin release as a control for probe placement, and only data from experiments in which this evoked at least a threefold increase in vasopressin concentration were analysed. Brains were removed and cut for histological confirmation of microdialysis probe placement.

Vasopressin in microdialysates was measured after lyophilization as previously described (Landgraf *et al.* 1995; Paiva *et al.* 2017) by a sensitive and selective radioimmunoassay (detection limit: 0.1 pg sample^{-1}; cross-reactivity less than 0.7%, RIAgnosis, Sinzing, Germany). Samples for measurement were blind coded.

Statistics

Fos expression in the retina. Three groups were compared by the non-parametric Kruskall–Wallis test, followed by Mann–Whitney *U* test to test the hypotheses (a) that light activates Fos expression in VP-RGCs and (b) that expression is higher in the light than in the dark period.

Retinal vasopressin content. Two groups ($n = 7$) were compared to test the hypothesis that the vasopressin

content of the retina differs between dark and night. Values were compared by Student's two-tailed *t* test.

Fos expression in the SCN. First, we compared light-induced Fos expression in early *vs.* late night. In subsequent experiments we tested the hypothesis that a V1a antagonist would attenuate light-induced Fos expression in the late night. Fos-positive nuclei were counted in each SCN in three to five sections per rat, and the median calculated; to combine these for group values, the medians were log-transformed as their distributions were skewed; *n* values are animal means. Groups were compared with Student's one-tailed *t* test, as this experiment tested a predetermined unidirectional hypothesis.

Microdialysis. In the experiment shown in Fig. 7, the basal levels of vasopressin varied in a threefold range between experiments, and so all data were normalized to the concentration in the first basal sample. The normalized data (excluding the first basal sample) from the two groups were compared by a repeated measures ANOVA followed by pairwise tests, using Bonferroni's and Tukey's multiple comparisons test.

***In vivo* electrophysiology.** Two hypotheses were tested in separate experiments: that V1a antagonist attenuates SCN responses to light, and that it attenuates SCN responses to electrical stimulation of the optic nerve. Each of these was tested by a paired comparison of the (mean) response in control condition and the mean response after application of the antagonist, using a two-tailed Wilcoxon signed rank test.

Results

Characterization of VP-RGCs

Vasopressin content in the retina has been previously described, and vasopressin has been found (by immunocytochemistry) to be expressed in some cells in both the ganglion cell layer and the inner nuclear layer of the retina (Gauquelin *et al.* 1983; Djeridane, 1994; Moritoh *et al.* 2011). We studied these cells in a transgenic rat strain in which enhanced green fluorescent protein (eGFP) is expressed under the control of the vasopressin promoter (Fig. 1*A* and *B*) (Ueta *et al.* 2005). eGFP-expressing cells comprised about 1% of cells in the ganglion cell layer (1.07 ± 0.01% of 33 868 cells from 9 retinas), and were sparsely distributed across the whole retina. By immunocytochemistry, we established that all the eGFP-expressing cells that we examined in the retina also expressed vasopressin-associated neurophysin: this large peptide is part of the vasopressin precursor peptide (Fig. 1*C*). eGFP (and vasopressin neurophysin) was also expressed in some small cells in the inner nuclear layer, which contains interneurons that do not project out of the retina.

The VP-RGCs were heterogeneous in size. In the inner nuclear layer, most eGFP-expressing cells were small: a sample of 21 of these cells had a mean (SEM) cross-sectional area of 58 ± 2.6 μm^2 (range 48–85 μm^2). By contrast, in a sample of 43 eGFP-expressing cells in the ganglion cell layer, 25 small cells had a mean (SEM) cross-sectional area of 83 ± 2.7 μm^2 (range 62–99 μm^2), while the 10 largest cells had a mean (SEM) cross-sectional area of 291 ± 13.2 μm^2 (range 154–333 μm^2). Using triple immunohistochemistry, we found that many large (but not small) VP-RGCs co-expressed the vesicle glutamate transporter 2 (vGLUT-2), indicating that these cells use glutamate as a neurotransmitter (Fig. 1*E*) (Fujiyama *et al.* 2003). In mammals, melanopsin is found in intrinsically photosensitive RGCs that project to the SCN and plays a critical role in regulating circadian rhythms (Provencio *et al.* 2000; Hattar *et al.* 2002; Hankins *et al.* 2008). VP-RGCs were often closely juxtaposed to immunoreactive melanopsin cells (Fig. 1*F*). Of the small VP-RGCs, only one cell of 300 counted contained detectable immunoreactive melanopsin, but of the large VP-RGCs, 25% (21/80) co-expressed melanopsin. We found no co-localization of eGFP with calretinin, parvalbumin, tyrosine hydroxylase, glycine, choline acetyltransferase or GAD65/67 (Fig. 2*A* and *F*), which label known subpopulations of retinal interneurons (Marc & Jones, 2002).

The vasopressin–eGFP transgene encodes a modified vasopressin precursor with eGFP fused in-frame at the C terminus (Ueta *et al.* 2005; and D. Murphy, personal communication). The signal peptide, vasopressin and neurophysin portions of the precursor are intact, and may be expressed from the transgene, and thus the vasopressin-associated neurophysin in eGFP rats may reflect either endogenous expression or transgene-driven expression. We therefore confirmed the expression of vasopressin in retinal cells in wild-type rats using antibodies against vasopressin–neurophysin (see below), the presence of vasopressin mRNA in the retina by PCR (Figs 1*D* and 3*B*), and the production of vasopressin by radioimmunoassay. The vasopressin content of the retina in wild-type rats was higher in the late afternoon (ZT11) than in the early morning (ZT1; 25 ± 2.6 *vs.* 52 ± 8 pg per retina, *n* = 7 per group, *P* < 0.015), consistent with light-induced activation of synthesis.

Venus labelling

To visualize the axons of the VP-RGCs in wild-type rats, we made intravitreal injections of a recombinant adeno-associated virus (rAAV) that results in the expression of a fluorescent protein, Venus (Fig. 3*A* and *B*; Supplementary Video S1) or tdTomato, under the control of 1.9 kbp of the vasopressin promoter (Fig. 4). We confirmed the successful transfection of retinal vasopressin cells by immunohistochemistry (Fig. 3*B*) for

vasopressin neurophysin. This confirms that the large RCGs do indeed express the endogenous vasopressin gene, as the AAV vector does not contain vasopressin coding sequences.

Unlike the eGFP–vasopressin transgenic rats, where the eGFP is packaged inside the same vesicles as vasopressin

(Ueta *et al.* 2005), these fluorescent proteins are released into (and fill) the cytoplasm of the neurons allowing tracking of thin neurites (Knobloch *et al.* 2012). In the transfected retinas, we found Venus labelling in the ganglion cell layer but not in the inner nuclear layer (Fig. 3C and D). Only larger VP-RGCs expressed Venus;
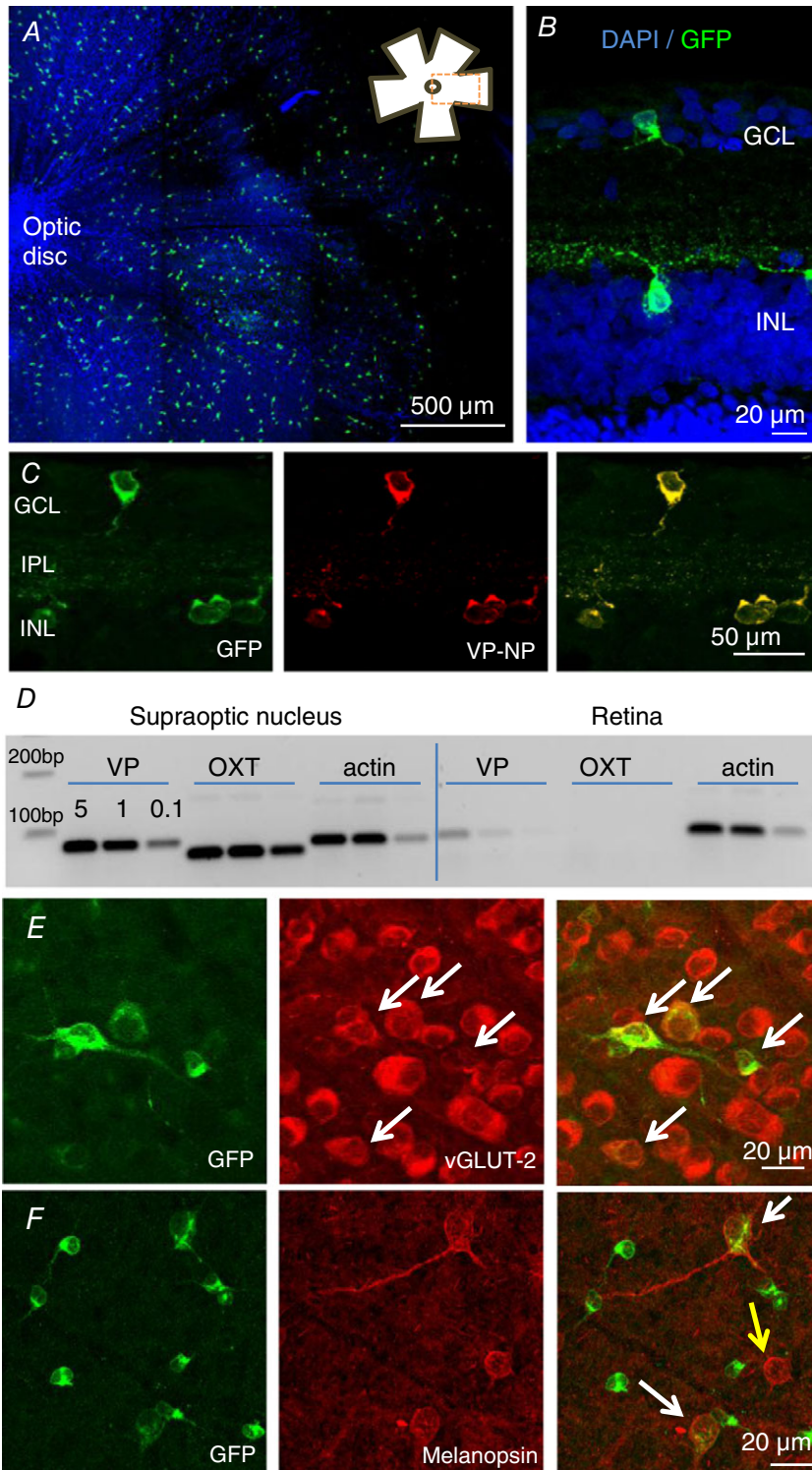
Figure 1. Vasopressin neurons in the retina
A, flat mount of retina, focused on the ganglion cell layer (GCL), shows dispersed eGFP-expressing cells (green cells); the blue staining is a nuclear marker DAPI, to show the location of all cells in the field of view; the inset shows the location of the image within the flat mount. *B*, eGFP-cells occur in both the ganglion cell layer (GCL) and the inner nuclear layer (INL), as shown in a cross section of the flat mount. *C*, eGFP-cells express vasopressin–neurophysin (VP-NP); the successive images show fluorescence for eGFP, immunoreactive VP-NP and overlaid images. *D*, PCR confirmation of expression of vasopressin mRNA (VP, 77 bp) and actin mRNA in the supraoptic nucleus (positive control) and the retina of wild-type rats; the supraoptic nucleus contains magnocellular neurons that project to the posterior pituitary gland. Note there is no detectable oxytocin mRNA (OXT, 62 bp) in the retina; oxytocin is a closely related peptide that is also expressed in the supraoptic nucleus. *E*, eGFP-cells (shown in a flat mount) co-express the vesicle glutamate transporter vGLUT-2 (white arrows) indicating that they use glutamate as a conventional neurotransmitter. *F*, some eGFP-cells co-express the photopigment melanopsin (white arrows; yellow arrow shows a cell immunopositive for melanopsin only).

no Venus was found in the small cells either in the inner nuclear layer or in the ganglion cell layer. In three retinas we sampled 220 Venus-labelled cells and 113 melanopsin-labelled cells; 45% of the Venus-labelled cells contained immunoreactive melanopsin and 88% of the melanopsin cells contained Venus, suggesting that most melanopsin-containing cells express vasopressin. We traced the passage of Venus-labelled axons into the optic nerve (Fig. 3*E*), and found a dense plexus in the ventro-lateral SCN (Fig. 3*F*). Using triple immunohistochemistry for Venus, vGLUT-2 and vasoactive intestinal polypeptide (VIP) or gastrin-releasing peptide (GRP) we found that 74% of VIP cells and 66% of GRP cells were apposed by boutons from Venus-labelled fibres (Fig. 3*I* and *J*). The Venus-labelled fibres co-expressed vGLUT-2 indicating that they were glutamatergic; as expected, vGLUT-2 was not co-expressed with either VIP or GRP, which are both

known to use GABA as a conventional neurotransmitter (Belenky *et al.* 2008).

We also found Venus-labelled fibres in the inter-geniculate leaflet (IGL), which is involved in regulation of circadian rhythms via its projections to the SCN (Hattar *et al.* 2006), and in the olivary pretectal nucleus (OPt), which controls the pupillary light reflex (Gamlin, 2006). However, we found no Venus-labelled fibres entering the superior colliculus, which is a major projection area of classical image-forming RGCs (Feinberg & Meister, 2015) (Fig. 4); some were found on the outskirts of the superior colliculus, but none were seen to enter this region. In two animals we transfected the right eye with AAV expressing Venus and the left eye with an AAV expressing tdTomato, both under the control of the vasopressin promoter. The labelled fibres terminated in the SCN, IGL and OPt (Fig. 4); most fibres were found at sites contralateral to the injected
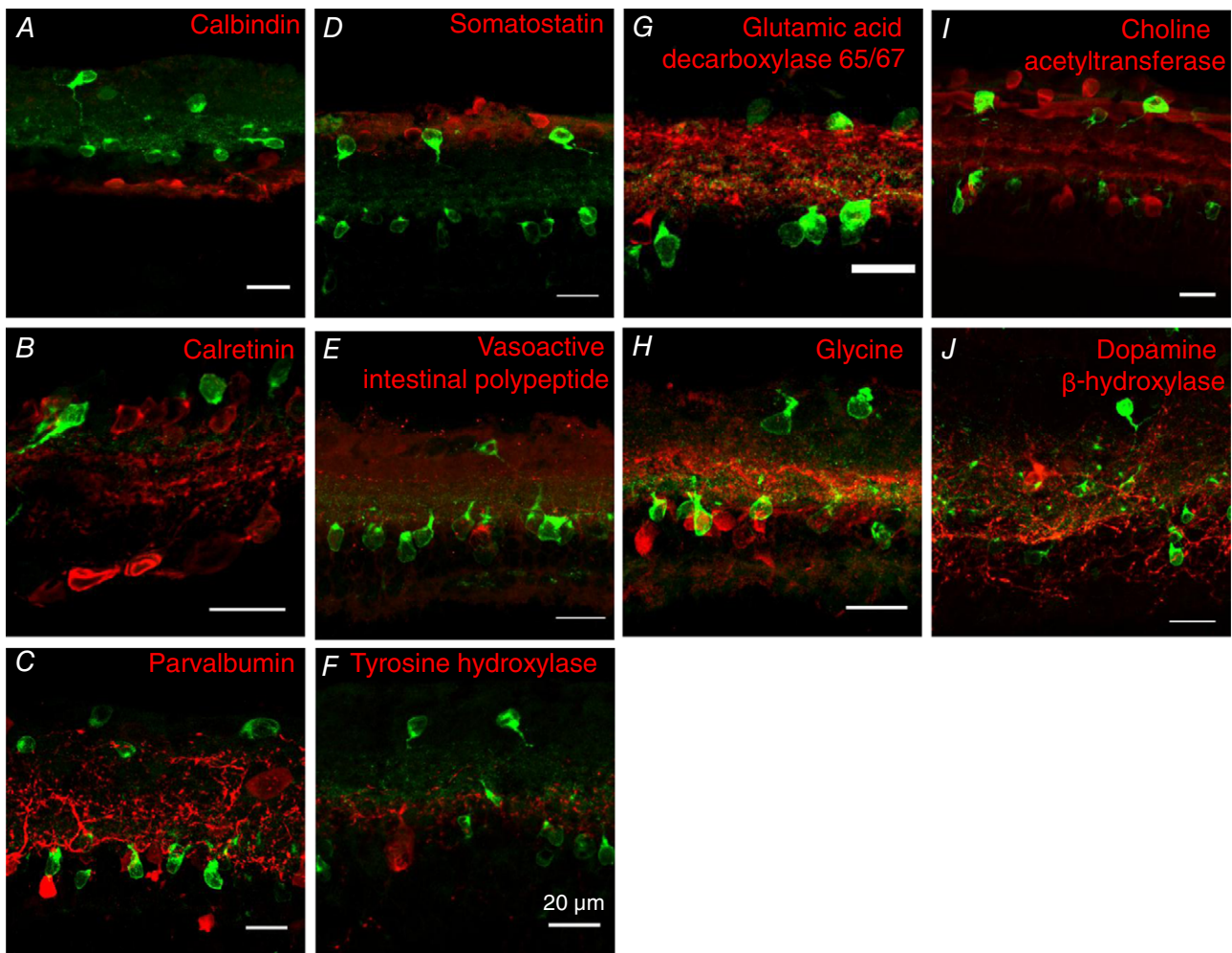

Figure 2. Vasopressin neurons in the retina
Immunohistochemistry for retinal cell types. Fluorescence immunohistochemistry showing that eGFP-expressing RGCs (green in top layer) and amacrine cells (green lower layer) do not co-express markers commonly used to identify retinal cells (red), including calcium binding proteins (*A–C*), neuropeptides (*D–F*) and 'classical' transmitters (*G–J*).
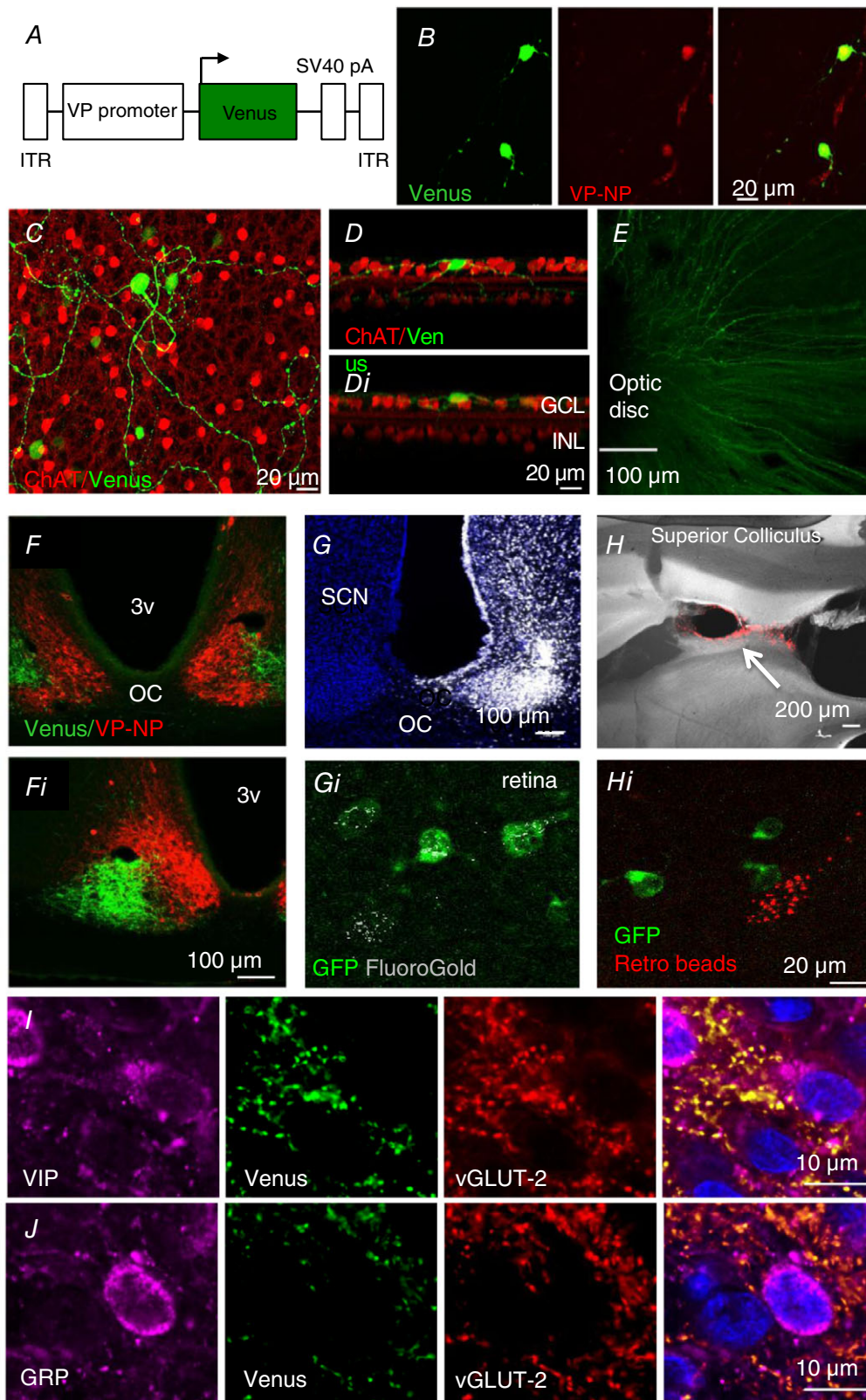
Figure 3. VP-RGC transfection and projections

A, scheme of the viral vector used to infect VP-RGCs. *B*, intravitreal injection in wild-type rats of an rAAV expressing Venus (green) under the control of the vasopressin promoter infects RGCs that express vasopressin–neurophysin (VP-NP, red; yellow in overlay). *C*, Venus labelling in a retinal flat mount. *D*, dendrites of RGCs branching into the

inner nuclear layer (INL) (*D*), or ganglion cell layer (GCL) (*Di*). *E*, Venus-labelled axonal projections converge on the optic disc, where the optic nerve leaves the retina. *F*, enlarged in *Fi*, the VP-RGCs project (green fibres; Venus) to the ventrolateral SCN; intrinsic vasopressin cells in red. *G* and *H*, retrograde tracer is found in some VP-RGCs (*Gi* and *Hi*) after microinjection into the SCN (*G*; fluorogold), but not after injection into the superior colliculus (*H*, Fluoro-Red beads). *I* and *J*, terminal boutons of Venus-labelled fibres in the SCN express vGLUT-2 and target vasoactive intestinal polypeptide (VIP; *I*) and gastrin-releasing peptide (GRP; *J*) cells. The blue staining is a nuclear marker, DAPI. 3V, 3rd ventricle; ITR, inverted terminal repeat sequence; OC, optic chiasm.

eye, but there was a substantial ipsilateral projection to the SCN in particular.

Retrograde tracing

We confirmed these projections by retrograde tracing studies (Fig. 3*G* and *H*). When retrograde tracer beads were injected into the SCN, IGL or OPt ($n = 2$–4 per area) we found labelling of large (but not small) eGFP-positive cells in the ganglion cell layer, and no labelling of any cells in the inner nuclear layer. We found no labelling after injections into the superior colliculus (Fig. 3*H*). To estimate how many of the RGCs that project to the SCN express vasopressin, we injected fluorogold into the SCN to fill this region completely (Fig. 3*G*). For the injection that achieved the best fill, we studied seven retinal sections with confocal microscopy. Of 176 melanopsin-labelled cells, 142 were retrogradely labelled with fluorogold; of these, 41 also expressed eGFP. In the same sections, we found only eight VP-RGCs that were labelled with fluorogold but which appeared to contain no melanopsin. These experiments confirmed that most of the retinal cells that project to the SCN contain immunoreactive melanopsin, and that vasopressin is expressed in a substantial subset of these cells and also in some cells that project to the SCN that did not apparently contain detectable amounts of immunoreactive melanopsin.

Light responsiveness of RGCs

To determine the response of VP-RGCs to light we measured the expression of the immediate early gene c-*fos* in the retina by immunocytochemical detection of Fos, the protein product of c-*fos*. In response to 1 h light stimulation of dark-adapted retinas (ZT21), there was a significant increase in Fos expression in VP-RGCs ($8.1 \pm 1.0\%$ of VP-RGCs expressed Fos after light exposure *vs.* $0.2 \pm 0.2\%$ with no light exposure; $n = 3$ and $n = 6$ respectively, $P = 0.0019$; Fig. 5*A* and *B*). Fos expression in VP-RGCs was even higher in retinas taken at ZT6 ($13.8 \pm 3.8\%$, $n = 6$), suggesting sustained expression of Fos in VP-RGCs throughout the day.

To characterize the responsiveness of VP-RGCs to light, we made *in vitro* patch-clamp recordings from 88 large RGCs identified by their expression of eGFP; 58 of these cells were transiently excited by light, and the other 30 were inhibited (Fig. 5*C* and *D*); previously, all immunoreactive melanopsin RGCs have been reported to

be excited by light (Schmidt *et al.* 2011). Current-clamp and voltage-clamp recordings from the light-activated VP-RGCs showed that afferent synaptic activity was increased during light stimulation, suggesting that activation was mediated at least partially by synaptic input (Fig. 5*F*). The close juxtaposition of the VP-RGCs to melanopsin cells indicates that they may receive these excitatory synaptic inputs from neighbouring, intrinsically photosensitive melanopsin cells (Schmidt *et al.* 2011; Hughes *et al.* 2016).

Vasopressin actions in the SCN

We then recorded the spike activity of single SCN neurons in urethane-anaesthetized rats (Tsuji *et al.* 2016). About two-thirds of light-responsive cells (150/222) were excited by light (5 s pulses) and about one-third were inhibited. In 10 cells excited by light (each from a different rat), responses were measured before and after injection of aCSF and after injection of a vasopressin V1a receptor antagonist into the third ventricle. The light-induced activation was unaffected by aCSF injection but was reduced by $30 \pm 8\%$ after antagonist injection (Wilcoxon matched pairs signed rank test; $P = 0.004$; Fig. 6*F*). We also tested the responses of SCN neurons to electrical stimulation of the retino-hypothalamic tract (RHT; 5 s trains at 50 Hz) (Fig. 6*A* and *E*). Seven SCN neurons (from seven rats) showed a prolonged excitatory response (for 3–7 s after stimulation) that was attenuated by I.C.V. injection of the V1a antagonist (Fig. 6*E*).

A short light pulse, given during the subjective night, induces Fos expression in the SCN, and this correlates with the ability of light to phase-shift activity–rest cycles (Fig. 7) (Ding *et al.* 1994). Consistent with previous studies, 60 min of light exposure at Z21 induced robust Fos expression in the SCN, and this activation was significantly greater than that induced by the same light exposure given at ZT15 (Fig. 7*B*). In separate experiments, rats were chronically infused I.C.V. with the V1a antagonist or vehicle via a subcutaneously implanted osmotic minipump connected to a cannula implanted in the lateral cerebral ventricle. Light-induced Fos expression at Z21 was significantly less in rats infused with the V1a antagonist (Fig. 7*A* and *C*) than in vehicle-infused rats.

Finally, we measured vasopressin release in the SCN (by microdialysis in urethane-anaesthetized rats) in response
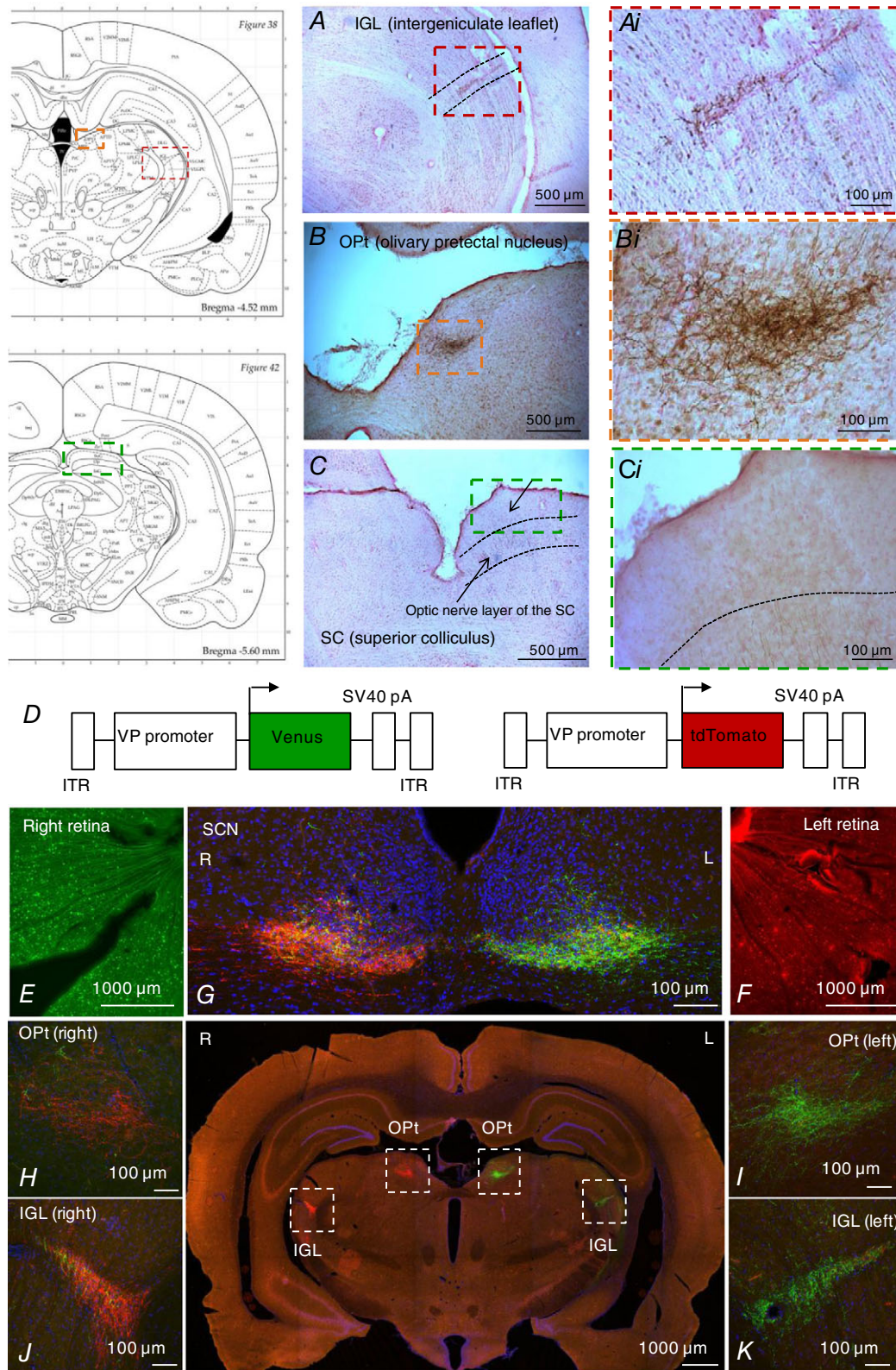
Figure 4. Projections of VP-RGCs

DAB immunohistochemistry in wild-type rats after intravitreal injection of an rAAV expressing Venus under the control of the vasopressin promoter into the retina shows some fibres projecting to the integeniculate leaflet (*A*) and olivary pretectal nucleus (*B*), but not to the superior colliculus (*C*). *D*, scheme of the viral vectors used to infect

VP-RGCs. Intravitreal injection of an rAAV expressing Venus (green) into the right retina (*E*) and tdTomato (red) into the left retina (*F*) shows that the fibres terminate in the SCN, intergeniculate leaflet (IGL) and olivary pretectal nucleus (OPt) with the majority contralateral to the injected eye (*G–K*).

to light exposure. In pilot experiments we found that application of light (1 min on, 1 min off for 40 min) to the contralateral eye at ZT6 increased vasopressin release in the SCN from 0.54 ± 0.14 to 1.76 ± 0.35 pg sample^{-1} in samples collected every 40 min ($n = 6$ per group, $P < 0.05$). In two further groups of rats, we collected 30 min samples at the beginning and end of subjective day before and after light was given for 30 min. The 'early morning' group was exposed to light at ZT3 after being maintained in the dark continuously after the preceding dark phase; the 'evening' group was exposed to light at

ZT12 after being maintained in the dark from ZT9, to ensure dark adaptation of light responsiveness. In the 'early morning' group, light exposure was followed by a significant increase in vasopressin concentration, whereas in the 'late evening' group, light exposure produced a significant decrease (Fig. 7*D*).

Discussion

The present study shows that vasopressin, well known to be an important output of the SCN (Kalsbeek *et al.* 2010), is
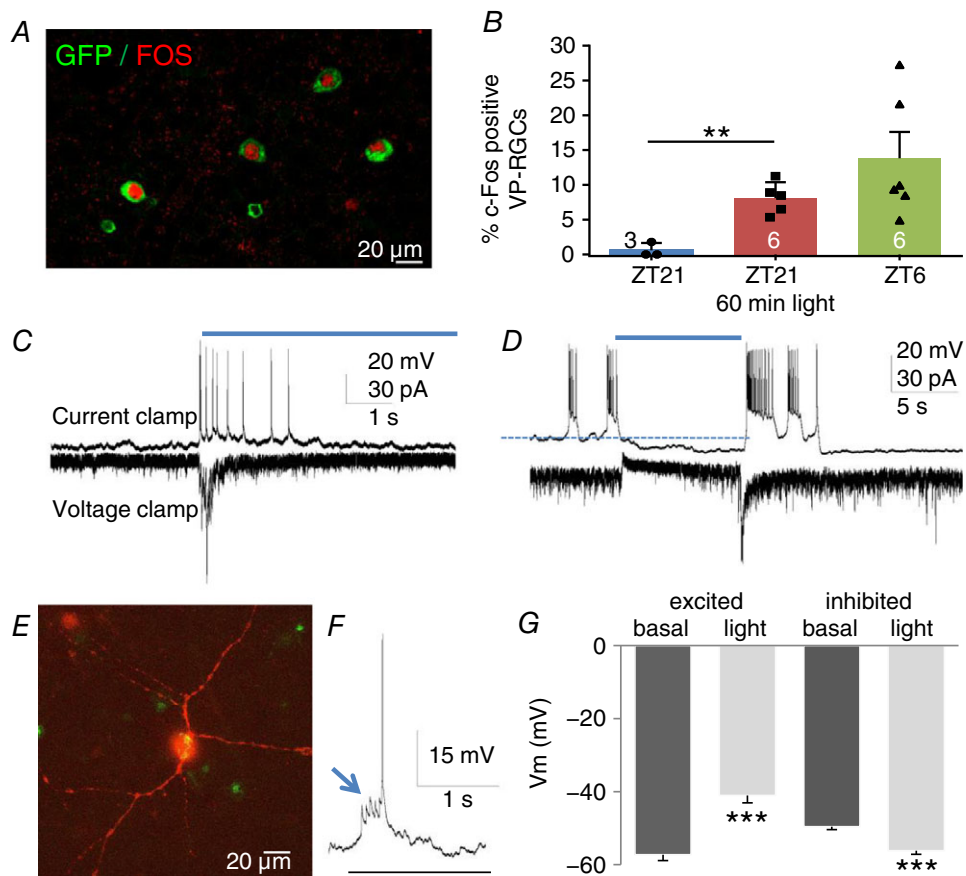

Figure 5. Light exposure excites VP-RGCs
A, the expression of Fos in VP-RGCs in the day (ZT6). *B*, expression is higher in the day (ZT6) than in the dark (ZT21) and is induced by light stimulation in the dark (mean difference, 7.5; 95% CI, 4.0 to 11.0; **$P = 0.0019$). Patch-clamp recordings of VP-RGCs showing examples of a transient increase in spike activity during light exposure (*C*), and inhibition of spike activity (*D*). *E*, example of a patch-clamp recorded eGFP-labelled RGC filled with biocytin (red; overlay with green gives the yellow signal in the soma). *F*, spikes in response to light are initiated by excitatory postsynaptic potentials (arrow). *G*, summary of electrophysiology data showing changes in voltage potential (V_m, for stimulated (mean difference, 16.2; 95% CI, 12.8 to 19.6; ***$P = 0.0001$) and inhibited neurons (mean difference, -6.56; 95% CI, -7.9 to -5.2; ***$P = 0.0001$), $n = 58$ excited cells, 30 inhibited cells, means + SEM; ***$P < 0,001$). For source data in *B*, see Table S1; for source data in *G*, see Table S2.

also a time-dependent mediator of light information from the retina to the SCN, and so is likely to contribute to the effects of vasopressin on jet lag (Yamaguchi *et al.* 2013). The expression of neuropeptides in this projection has clear functional significance. These cells use glutamate as a neurotransmitter, secreted from small synaptic vesicles. Because glutamate can be rapidly recycled, this signalling is constantly available. However, many of the RGCs that project to the SCN also contain the neuropeptide pituitary adenylate cyclase-activating peptide (PACAP; Hattar *et al.* 2002; Schmidt *et al.* 2011), or as described here, vasopressin. At present, we do not know whether vasopressin and PACAP are co-expressed or are in separate populations of RGCs. Neuropeptides are not contained in the same vesicles as glutamate, but are packaged in separate, large vesicles that are synthesized at the cell body and transported along the axons (Burbach *et al.* 2001): these vesicles cannot be recycled as small synaptic vesicles are. Light stimulation rapidly induces Fos expression in VP-RGCs, and induction of Fos expression is implicated in the regulation of neuronal vasopressin synthesis (Cunningham *et al.* 2004). Thus, it is likely that, in VP-RGCs, Fos expression is linked to up-regulation of

peptide synthesis to replenish what has been released from the terminals. However, the path length from retina to SCN in the rat is >20 mm, and (in magnocellular vasopressin neurons) vasopressin-containing vesicles are transported along axons at only ~140 mm day^{-1} (Burbach *et al.* 2001). Given this, and given the delays between stimulation and production of new vesicles, the depletion of peptide by light-induced activation of release in the SCN cannot be replenished without a lag time of several hours. Thus, at the terminals in the SCN, the availability of peptide for release must be subject to a diurnal cycle of depletion and replenishment.

We have shown here that light given at the end of the dark phase consistently evokes measurable vasopressin release in the SCN, whereas light given at the beginning of the dark phase does not. We predicted that light stimulation would increase vasopressin release from retinal afferents, and would excite a majority of the first order recipient neurons in the SCN. The retinal afferents do innervate predominantly VIP and GRP neurons, but do not directly innervate the intrinsic vasopressin cells of the SCN, which are regulated by inhibitory GABAergic projections by the retinal recipient neurons. However,
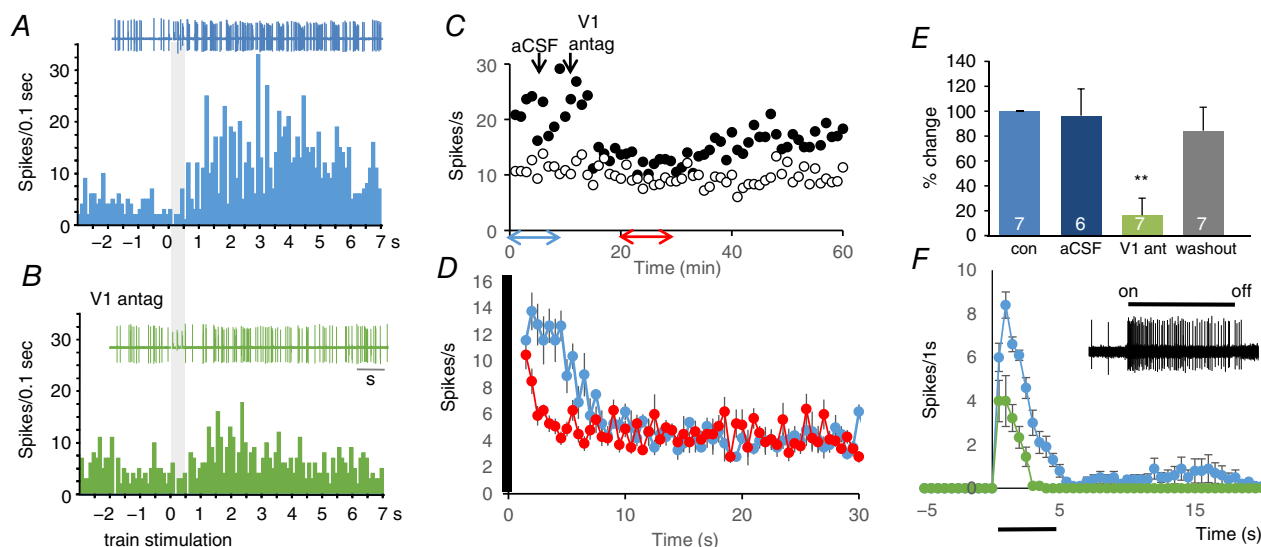

Figure 6. Vasopressin effects on SCN cells

A and *B*, I.C.V. injection of a vasopressin V1a antagonist blocks the response of an SCN neuron *in vivo* to electrical stimulation of the RHT (grey bar), shown in post-stimulus time histograms before (*A*) and after (*B*) antagonist injection. *C*, example of the response of an SCN cell to repeated electrical stimulation of the RHT; the filled circles plot the number of spikes recorded in the 6 s after stimulation of the RHT for 0.5 s at 50 Hz delivered every minute; the open circles plot the number of spikes in the following 6 s. A V1a antagonist given I.C.V. (arrow) markedly attenuates the response to stimulation for about 20 min after a lag of 3 min. *D*, mean (SEM) response to RHT stimulation of the same cell, shown in blue for the first 10 responses plotted in *C* and in red for the 10 responses plotted between 20 and 30 min in *C*. *E*, mean responses to RHT stimulation of 7 SCN cells plotted as percentage differences from control firing rate after I.C.V. injection of aCSF followed by I.C.V. injection of the V1a antagonist and after recovery (washout) (***$P = 0.009$ *vs.* control; two-tailed Wilcoxon signed rank test; numbers in columns are *n*/group). *F*, I.C.V. injection of antagonist attenuates the responses of SCN neuron *in vivo* to light: this panel shows the response of a representative SCN neuron to light; it shows the mean (SEM) responses to repeated light exposures before and after injection of the antagonist (*n* = 9 in each case). For source data in *E* see Table S3; for source data in *F*, see Table S4.
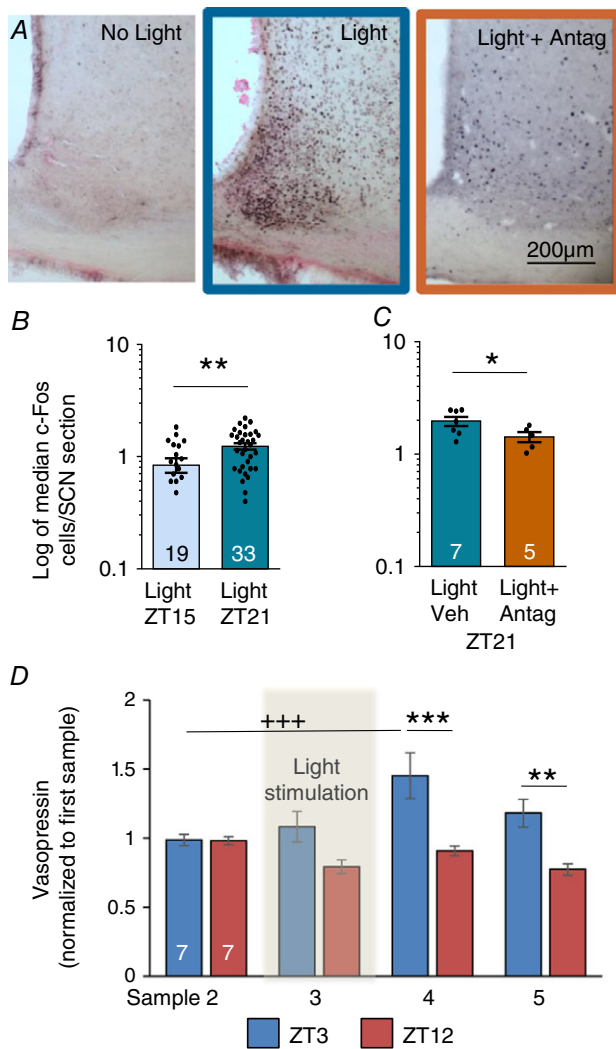
Figure 7. Vasopressin effects on SCN Fos expression

A, hypothalamic sections at the level of the SCN stained for Fos (black nuclear stain), and lightly counterstained with nuclear fast red. A 60 min light pulse presented at the beginning of the dark period (ZT15) induces more Fos expression in the SCN than a pulse presented towards the end of the dark period (ZT21). Light-induced Fos expression is attenuated by a vasopressin V1a antagonist. *B*, data (median numbers of Fos cells counted per SCN section) from all individual animals are given as points (mean difference, 0.39; 95% CI, 0.1 to 0.68; **$P = 0.0095$). *C*, data (median numbers of Fos cells counted per SCN section) from all individual animals are given as points (mean difference, 0.54; 95% CI, −1.1 to 0.02; **$P = 0.029$). *D*, light stimulation increases the vasopressin content in SCN microdialysates in the 'early morning' group (light exposure at ZT3) but not the 'evening' group (light at ZT12) as measured by radioimmunoassay (RM ANOVA followed by Bonferroni's and Tukey's multiple comparisons tests). Mean difference, 0.54; 95% CI, 0.23 to 0.85; ***$P = 0.0001$; mean difference, 0.41; 95% CI, 0.1 to 0.72; **$P = 0.005$; mean difference, −0.47; 95% CI, −0.75 to −0.18; +++$P = 0.0006$. Bars show means + SEM. Numbers in columns are *n* per group. For source data in *B* see Table S5; for source data in *C*, see Table S6; for source data in *D*, see Table S7.

some of the retinal recipient neurons are inhibited by light, so there may be activation of intrinsic vasopressin cells from these inputs. In addition, it has been suggested that GABA may excite some SCN vasopressin neurons (Belenky *et al.* 2010). Thus, how much of the vasopressin collected in the microdialysates is released from the retina projection or released from the endogenous population of SCN vasopressin neurons in response to light stimulation is unclear. SCN vasopressin neurons project to the paraventricular nucleus of the hypothalamus, the subparaventricular zone, medial preoptic area, and into the contralateral SCN. SCN vasopressin neurons have also axon collaterals that remain inside the boundaries of the SCN (Pennartz *et al.* 1998) and release vasopressin from their somata and dendrites (Castel *et al.* 1996).

We have also shown that light-induced Fos expression in the SCN is higher at the end of the night than earlier, and SCN Fos expression has been linked to light-induced phase shifts. Accordingly, cyclical availability of neuropeptides for release may explain why a light pulse given close to the end of the night is more likely to result in a phase advance of circadian rhythms than one given earlier.

Exactly why light is so ineffective at eliciting Fos expression in the early part of the dark phase remains intriguing; even if the retinal terminals are depleted of vasopressin they should still be releasing glutamate in response to light. The answer may simply be that, although c-fos is often thought of as an indiscriminate marker of neuronal excitation, this is over-simplistic: in magnocellular oxytocin neurons for example, the neuropeptide α-melanocyte-stimulating hormone (α-MSH) induces Fos expression but inhibits neuronal activity (Sabatier *et al. et al.* 2003), while antidromic stimulation of increased spike activity is completely ineffective at increasing Fos expression (Luckman *et al.* 1994). The likely mechanistic link between synaptic activation appears to be via increased intracellular calcium, and as vasopressin is a potent mobilizer of intracellular calcium stores (Sabatier *et al.* 1998), it may be a particularly potent inducer of Fos expression.

Vasopressin is involved in diverse physiological and behavioural processes; vasopressin secreted from the pituitary gland is essential for fluid and electrolyte balance, but vasopressin released within the brain has many roles, including in social behaviour, in aggression and in behavioural rhythms. Vasopressin is an important output of the SCN; its secretion into the CSF peaks in the early morning and declines by late afternoon (Kalsbeek *et al.* 2010), and its targets include vasopressin cells in other parts of the hypothalamus. In particular, vasopressin released from the SCN during late sleep activates osmosensory afferents to the vasopressin neurons in the supraoptic nucleus (Trudel & Bourque, 2010) and to neurons in the organum vasculosum of

the lamina terminalis (Gizowski *et al.* 2016). Supraoptic neurons secrete vasopressin from nerve terminals in the posterior pituitary, which acts on the kidneys to concentrate the urine. Regulation of this antidiuretic system by the SCN suppresses nocturnal enuresis, and is important in maintaining sleep (Gizowski *et al.* 2016). Magnocellular vasopressin neurones of the supraoptic nucleus also directly control a diversity of behavioural processes, via central axonal projections and via extensive dendritic secretion of vasopressin (Ludwig & Leng, 2006; Neumann & Landgraf, 2012; Stoop, 2012). Thus although vasopressin is expressed at several sites in the nervous system as well as in the retina, it appears that some of these vasopressin neurons are linked in functionally coherent chains to integrate multiple physiological and behavioural functions.

Shift work that includes a night-time rotation and long-distance travel has become an unavoidable attribute of today's 24 h society. The related disruption of the human circadian time organization leads in the short term to an array of jet lag-like symptoms, and in the long run it contributes to weight gain and obesity, metabolic syndrome, type II diabetes and cardiovascular disease. Studies suggest increased cancer risk, symptoms of insomnia, depression, elevated cortisol levels, cognitive impairment and premature mortality (Hastings *et al.* 2003; Froy, 2011; Kondratova & Kondratov, 2012). The mechanisms leading to circadian dysfunction are largely unknown. The reported association of vasopressin with jet lag (Yamaguchi *et al.* 2013) raises the interesting possibility that interventions in vasopressin signalling from the retina may have important therapeutic benefits.

References

Albrecht U (2012). Timing to perfection: the biology of central and peripheral circadian clocks. *Neuron* **74**, 246–260.

Antle MC, Smith VM, Sterniczuk R, Yamakawa GR & Rakai BD (2009). Physiological responses of the circadian clock to acute light exposure at night. *Rev Endocr Metab Disord* **10**, 279–291.

Belenky MA, Sollars PJ, Mount DB, Alper SL, Yarom Y & Pickard GE (2010). Cell-type specific distribution of chloride transporters in the rat suprachiasmatic nucleus. *Neuroscience* **165**, 1519–1537.

Belenky MA, Yarom Y & Pickard GE (2008). Heterogeneous expression of gamma-aminobutyric acid and gamma-aminobutyric acid-associated receptors and transporters in the rat suprachiasmatic nucleus. *J Comp Neurol* **506**, 708–732.

Berson DM, Dunn FA & Takao M (2002). Phototransduction by retinal ganglion cells that set the circadian clock. *Science* **295**, 1070–1073.

Bielsky IF, Hu SB, Ren X, Terwilliger EF & Young LJ (2005). The V1a vasopressin receptor is necessary and sufficient for normal social recognition: a gene replacement study. *Neuron* **47**, 503–513.

Bosch OJ & Neumann ID (2012). Both oxytocin and vasopressin are mediators of maternal care and aggression in rodents: from central release to sites of action. *Horm Behav* **61**, 293–303.

Burbach JP, Luckman SM, Murphy D & Gainer H (2001). Gene regulation in the magnocellular hypothalamo-neurohypophysial system. *Physiol Rev* **81**, 1197–1267.

Castel M, Morris J & Belenky M (1996). Non-synaptic and dendritic exocytosis from dense-cored vesicles in the suprachiasmatic nucleus. *Neuroreport* **7**, 543–547.

Chiu K, Chang RC & So KF (2007). Intravitreous injection for establishing ocular diseases model. *J Vis Exp* 313.

Cunningham JT, Penny ML & Murphy D (2004). Cardiovascular regulation of supraoptic neurons in the rat: synaptic inputs and cellular signals. *Prog Biophys Mol Biol* **84**, 183–196.

Dijk F, Kraal-Muller E & Kamphuis W (2004). Ischemia-induced changes of AMPA-type glutamate receptor subunit expression pattern in the rat retina: a real-time quantitative PCR study. *Invest Ophthalmol Vis Sci* **45**, 330–341.

Ding JM, Chen D, Weber ET, Faiman LE, Rea MA & Gillette MU (1994). Resetting the biological clock: mediation of nocturnal circadian shifts by glutamate and NO. *Science* **266**, 1713–1717.

Djeridane Y (1994). Immunohistochemical evidence for the presence of vasopressin in the rat harderian gland, retina and lacrimal gland. *Exp Eye Res* **59**, 117–120.

Donaldson ZR & Young LJ (2008). Oxytocin, vasopressin, and the neurogenetics of sociality. *Science* **322**, 900–904.

During MJ, Young D, Baer K, Lawlor P & Klugmann M (2003). Development and optimization of adeno-associated virus vector transfer into the central nervous system. *Methods Mol Med* **76**, 221–236.

Feinberg EH & Meister M (2015). Orientation columns in the mouse superior colliculus. *Nature* **519**, 229–232.

Froy O (2011). Circadian rhythms, aging, and life span in mammals. *Physiology (Bethesda)* **26**, 225–235.

Fujiyama F, Hioki H, Tomioka R, Taki K, Tamamaki N, Nomura S, Okamoto K & Kaneko T (2003). Changes of immunocytochemical localization of vesicular glutamate transporters in the rat visual system after the retinofugal denervation. *J Comp Neurol* **465**, 234–249.

Gainer H, Ponzio TA, Yue C & Kawasaki M (2011). Intron-specific neuropeptide probes. *Methods Mol Biol* **789**, 89–110.

Gamlin PD (2006). The pretectum: connections and oculomotor-related roles. *Prog Brain Res* **151**, 379–405.

Gauquelin G, Geelen G, Louis F, Allevard AM, Meunier C, Cuisinaud G, Benjanet S, Seidah NG, Chretien M, Legros JJ & Gharib C (1983). Presence of vasopressin, oxytocin and neurophysin in the retina of mammals, effect of light and darkness, comparison with the neuropeptide content of the neurohypophysis and the pineal gland. *Peptides* **4**, 509–515.

Gizowski C, Zaelzer C & Bourque CW (2016). Clock-driven vasopressin neurotransmission mediates anticipatory thirst prior to sleep. *Nature* **537**, 685–688.

Golombek DA & Rosenstein RE (2010). Physiology of circadian entrainment. *Physiol Rev* **90**, 1063–1102.

Hankins MW, Peirson SN & Foster RG (2008). Melanopsin: an exciting photopigment. *Trends Neurosci* **31**, 27–36.

Hastings MH, Reddy AB & Maywood ES (2003). A clockwork web: circadian timing in brain and periphery, in health and disease. *Nat Rev Neurosci* **4**, 649–661.

Hattar S, Kumar M, Park A, Tong P, Tung J, Yau KW & Berson DM (2006). Central projections of melanopsin-expressing retinal ganglion cells in the mouse. *J Comp Neurol* **497**, 326–349.

Hattar S, Liao HW, Takao M, Berson DM & Yau KW (2002). Melanopsin-containing retinal ganglion cells: architecture, projections, and intrinsic photosensitivity. *Science* **295**, 1065–1070.

Hughes S, Jagannath A, Rodgers J, Hankins MW, Peirson SN & Foster RG (2016). Signalling by melanopsin (OPN4) expressing photosensitive retinal ganglion cells. *Eye (Lond)* **30**, 247–254.

Kalsbeek A, Fliers E, Hofman MA, Swaab DF & Buijs RM (2010). Vasopressin and the output of the hypothalamic biological clock. *J Neuroendocrinol* **22**, 362–372.

Knobloch HS, Charlet A, Hoffmann LC, Eliava M, Khrulev S, Cetin AH, Osten P, Schwarz MK, Seeburg PH, Stoop R & Grinevich V (2012). Evoked axonal oxytocin release in the central amygdala attenuates fear response. *Neuron* **73**, 553–566.

Kondratova AA & Kondratov RV (2012). The circadian clock and pathology of the ageing brain. *Nat Rev Neurosci* **13**, 325–335.

Kornhauser JM, Mayo KE & Takahashi JS (1996). Light, immediate-early genes, and circadian rhythms. *Behav Genet* **26**, 221–240.

Kruszynski M, Lammek B, Manning M, Seto J, Haldar J & Sawyer WH (1980). [l-(β-Mercapto-β,β-cyclopentamethylene propionic acid), 2-(O-methyl) tyrosine] arginine-vasopressin and [l-(β-mercapto-β, β-cyclopentamethylene propionic acid)], two highly potent antagonists of the vasopressor response to arginine vasopressin. *J Med Chem* **23**, 364–368.

Landgraf R, Neumann I, Holsboer F & Pittman QJ (1995). Interleukin-1β stimulates both central and peripheral release of vasopressin and oxytocin in the rat. *Eur J Neurosci* **7**, 592–598.

LeGates TA, Fernandez DC & Hattar S (2014). Light as a central modulator of circadian rhythms, sleep and affect. *Nat Rev Neurosci* **15**, 443–454.

Li JD, Burton KJ, Zhang C, Hu SB & Zhou QY (2009). Vasopressin receptor V1a regulates circadian rhythms of locomotor activity and expression of clock-controlled genes in the suprachiasmatic nuclei. *Am J Physiol Regul Integr Comp Physiol* **296**, R824–R830.

Lucas RJ (2013). Mammalian inner retinal photoreception. *Curr Biol* **23**, R125–R133.

Luckman SM, Dyball RE & Leng G (1994). Induction of c-fos expression in hypothalamic magnocellular neurons requires synaptic activation and not simply increased spike activity. *J Neurosci* **14**, 4825–4830.

Ludwig M & Leng G (2006). Dendritic peptide release and peptide-dependent behaviours. *Nat Rev Neurosci* **7**, 126–136.

Ludwig M, Sabatier N, Bull PM, Landgraf R, Dayanithi G & Leng G (2002). Intracellular calcium stores regulate activity-dependent neuropeptide release from dendrites. *Nature* **418**, 85–89.

Marc RE & Jones BW (2002). Molecular phenotyping of retinal ganglion cells. *J Neurosci* **22**, 413–427.

Masland RH (2001). The fundamental plan of the retina. *Nat Neurosci* **4**, 877–886.

Mieda M, Ono D, Hasegawa E, Okamoto H, Honma K, Honma S & Sakurai T (2015). Cellular clocks in AVP neurons of the SCN are critical for interneuronal coupling regulating circadian behavior rhythm. *Neuron* **85**, 1103–1116.

Moritoh S, Sato K, Okada Y & Koizumi A (2011). Endogenous arginine vasopressin-positive retinal cells in arginine vasopressin-eGFP transgenic rats identified by immunohistochemistry and reverse transcriptase-polymerase chain reaction. *Mol Vis* **17**, 3254–3261.

Neumann ID & Landgraf R (2012). Balance of brain oxytocin and vasopressin: implications for anxiety, depression, and social behaviors. *Trends Neurosci* **35**, 649–659.

Paiva L, Sabatier N, Leng G & Ludwig M (2017). Effect of melanotan-II on brain fos immunoreactivity and oxytocin neuronal activity and secretion in rats. *J Neuroendocrinol* **29**, doi: 10.1111/jne.12454.

Paxinos G & Watson C (2006). *The Rat Brain in Stereotaxic Coordinates*. Academic Press, San Diego.

Pennartz CM, Bos NP, Jeu MT, Geurtsen AM, Mirmiran M, Sluiter AA & Buijs RM (1998). Membrane properties and morphology of vasopressin neurons in slices of rat suprachiasmatic nucleus. *J Neurophysiol* **80**, 2710–2717.

Porterfield VM & Mintz EM (2009). Temporal patterns of light-induced immediate-early gene expression in the suprachiasmatic nucleus. *Neurosci Lett* **463**, 70–73.

Provencio I, Rodriguez IR, Jiang G, Hayes WP, Moreira EF & Rollag MD (2000). A novel human opsin in the inner retina. *J Neurosci* **20**, 600–605.

Reppert SM & Weaver DR (2002). Coordination of circadian timing in mammals. *Nature* **418**, 935–941.

Rusak B, Abe H, Mason R, Piggins HD & Ying SW (1993). Neurophysiological analysis of circadian rhythm entrainment. *J Biol Rhythms* **8** Suppl, S39–S45.

Sabatier N, Caquineau C, Dayanithi G, Bull P, Douglas AJ, Guan XM, Jiang M, Van der Ploeg L & Leng G (2003). α-Melanocyte-stimulating hormone stimulates oxytocin release from the dendrites of hypothalamic neurons while inhibiting oxytocin release from their terminals in the neurohypophysis. *J Neurosci* **23**, 10351–10358.

Sabatier N, Richard P & Dayanithi G (1998). Activation of multiple intracellular transduction signals by vasopressin in vasopressin-sensitive neurones of the rat supraoptic nucleus. *J Physiol* **513**, 699–710.

Saeb-Parsy K & Dyball RE (2003). Responses of cells in the rat suprachiasmatic nucleus in vivo to stimulation of afferent pathways are different at different times of the light/dark cycle. *J Neuroendocrinol* **15**, 895–903.

Schmidt TM, Chen SK & Hattar S (2011). Intrinsically photosensitive retinal ganglion cells: many subtypes, diverse functions. *Trends Neurosci* **34**, 572–580.

Schmidt TM & Kofuji P (2011). An isolated retinal preparation to record light response from genetically labeled retinal ganglion cells. *J Vis Exp* 2367.

Son SJ, Filosa JA, Potapenko ES, Biancardi VC, Zheng H, Patel KP, Tobin VA, Ludwig M & Stern JE (2013). Dendritic peptide release mediates interpopulation crosstalk between neurosecretory and preautonomic networks. *Neuron* **78**, 1036–1049.

Stoop R (2012). Neuromodulation by oxytocin and vasopressin. *Neuron* **76**, 142–159.

Subburaju S & Aguilera G (2007). Vasopressin mediates mitogenic responses to adrenalectomy in the rat anterior pituitary. *Endocrinology* **148**, 3102–3110.

Tobin VA, Hashimoto H, Wacker DW, Takayanagi Y, Langnaese K, Caquineau C, Noack J, Landgraf R, Onaka T, Leng G, Meddle SL, Engelmann M & Ludwig M (2010). An intrinsic vasopressin system in the olfactory bulb is involved in social recognition. *Nature* **464**, 413–417.

Trudel E & Bourque CW (2010). Central clock excites vasopressin neurons by waking osmosensory afferents during late sleep. *Nat Neurosci* **13**, 467–474.

Tsuji T, Tsuji C, Ludwig M & Leng G (2016). The rat suprachiasmatic nucleus: the master clock ticks at 30 Hz. *J Physiol* **594**, 3629–3650.

Ueta Y, Fujihara H, Serino R, Dayanithi G, Ozawa H, Matsuda K, Kawata M, Yamada J, Ueno S, Fukuda A & Murphy D (2005). Transgenic expression of enhanced green fluorescent protein enables direct visualization for physiological studies of vasopressin neurons and isolated nerve terminals of the rat. *Endocrinology* **146**, 406–413.

Yamaguchi Y, Suzuki T, Mizoro Y, Kori H, Okada K, Chen Y, Fustin JM, Yamazaki F, Mizuguchi N, Zhang J, Dong X, Tsujimoto G, Okuno Y, Doi M & Okamura H (2013). Mice genetically deficient in vasopressin V1a and V1b receptors are resistant to jet lag. *Science* **342**, 85–90.

Additional information

Competing interests

The authors declare that there are no conflicts of interest.

Funding information

Acknowledgements

Author contributions

M.L. and G.L.: conception and design, acquisition of data, analysis and interpretation of data, drafting or revising the article; V.G. and J.E.S.: conception and design, analysis and interpretation of data; T.T., A.J.A., M.Z., C.T., V.A.T., R.P. and A.R.: acquisition of data, analysis and interpretation of data. All authors have approved the final version of the manuscript and agree to be accountable for all aspects of the work. All persons designated as authors qualify for authorship, and all those who qualify for authorship are listed.

Supporting information

The following supporting information is available in the online version of this article.

Video S1. Animation of confocal images, showing cumulative stacking of sequential z slices from a retina flat mount, providing a 3D representation of the dendritic arborization of Venus filled (green) vasopressin expressing retinal ganglion cells.

Table S1. Source data for Fig. 5*B*.
Table S2. Source data for Fig. 5*G*.
Table S3. Source data for Fig. 6*E*.
Table S4. Source data for Fig. 6*F*.
Table S5. Source data in Fig. 7*B*.
Table S6. Source data in Fig. 7*C*.
Table S7. Source data in Fig. 7*D*.